inorganics

MDPI

Supporting Information

Luminescent Zn Halide Complexes with 2-(2-aminophenyl)benzothiazole Derivatives

by Taisiya S. Sukhikh, Dmitry S. Kolybalov, Ekaterina K. Pylova and Sergey N. Konchenko

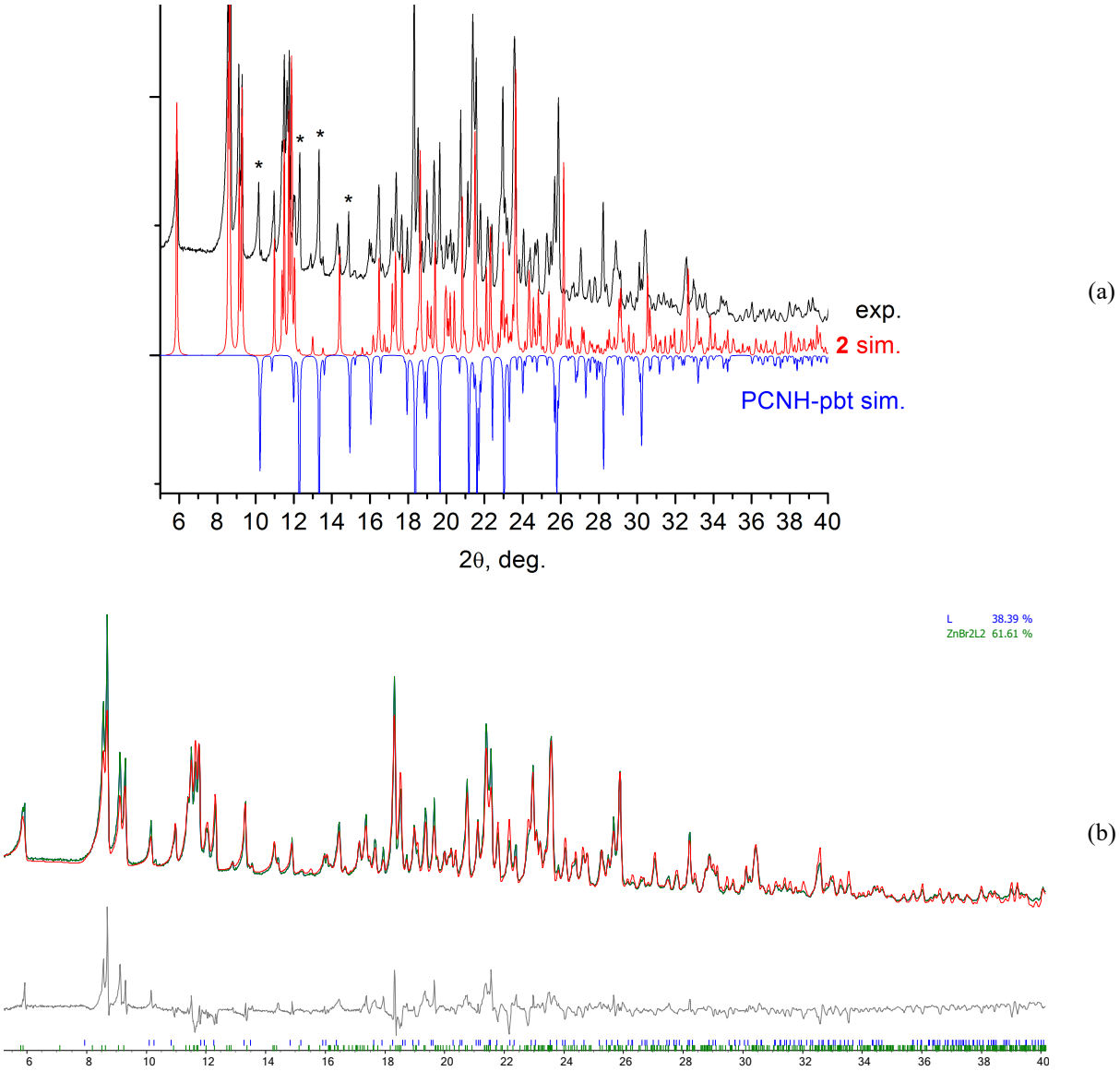

Figure S1. (**a**) Simulated powder XRD patterns (red for [Zn(L)$_2$Br$_2$] (**2**), blue for PCNH-*pbt*) and experimental (black) pattern for a sample from the reaction between ZnBr$_2$ and PCNH-*pbt* in a molar ratio of 1:2 (CuKα1 radiation). The most notable reflections of PCNH-*pbt* phase are highlighted by "*". (**b**) The corresponding Rietveld refinement of the experimental pattern (green) as a mixture of compounds PCNH-*pbt* and **2** (red) in a molar ratio of ca. 60/40% (mass ratio of 40/60%) and the difference (gray).

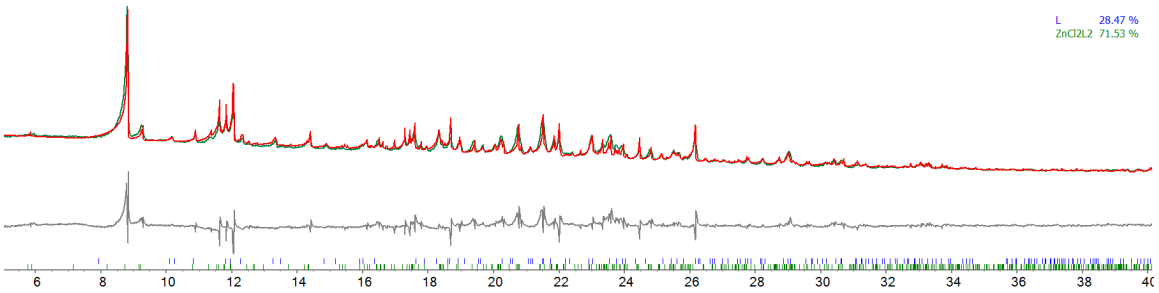

Figure S2. Experimental pattern (green) for a sample from the reaction between $ZnCl_2$ and PCNH-*pbt* in a molar ratio of 1:2 (CuKα1 radiation) and the Rietveld refinement as a mixture of compounds PCNH-*pbt* and **1** (red) in a molar ratio of ca. 45/55% (mass ratio of 28/72%) and the difference (gray).

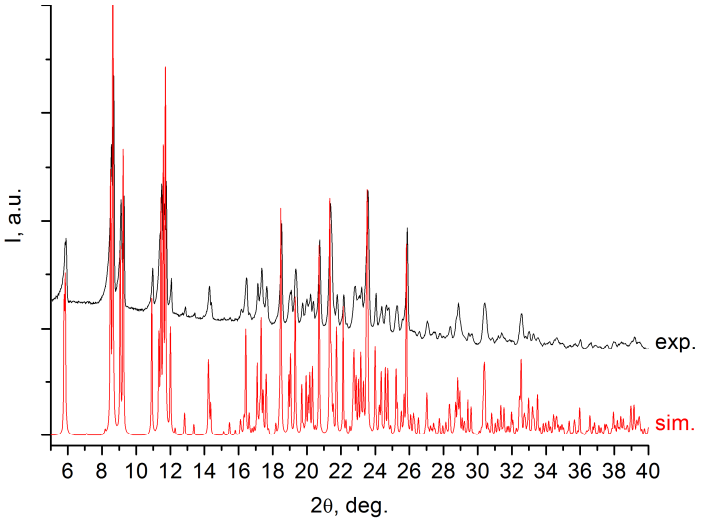

Figure S3. Simulated (red) and experimental (black) powder XRD patterns for the compound $[Zn(L)_2Br_2]$ (**2**; CuKα1 radiation).

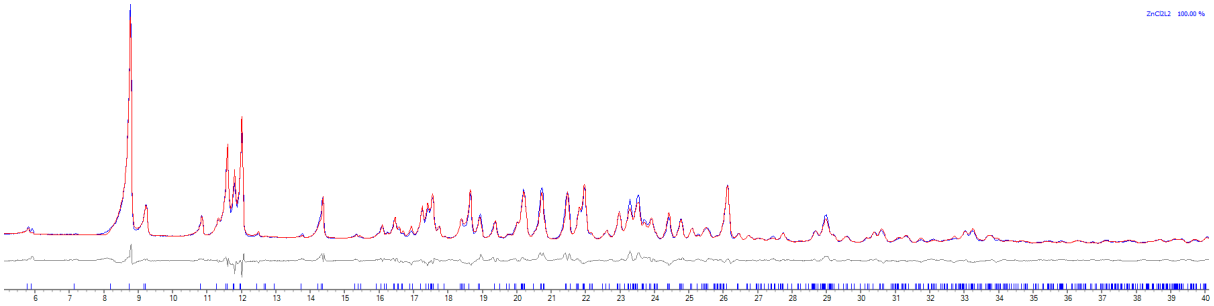

Figure S4. Rietveld refinement of powder XRD pattern for compound $[Zn(L)_2Cl_2]$ (**1**). Blue – experiment, red – fit, and gray – difference (CuKα1 radiation). Refined unit cell parameters: *P*–1, a = 11.5675(4) Å, b = 16.3410(7) Å, c = 16.3629(7) Å, α = 72.023(3)°, β = 71.243(3)°, γ = 75.210(4)°, V = 2743.6(2) Å^3. Positions of Cl atoms were refined to give reasonable Zn–Cl distances of 2.1–2.2 Å. Other atomic positions were fixed the same as in the single-crystal structure of $[Zn(L)_2Br_2]$ (**2**).

Table S1. Torsion angle N–C–C–C defining twist angle between thiazole and phenyl moieties, and hydrogen bond characteristics for compounds comprising NH-*pbt* moiety.

Compound 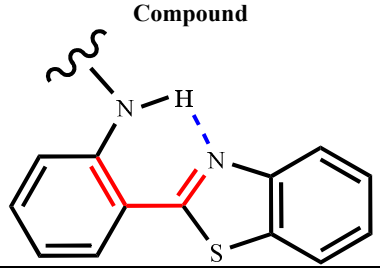	**N–C–C–C, deg.**	**N–H, Å**	**H···N, Å**	**N···N, Å**	**N–H···N, deg.**
$[Zn(L)_2Br_2]$ (**2**)	3.6(5), 15.0(7)	0.852(19), 0.88	2.05(3), 2.06	2.710(4), 2.729(5)	134(4), 132.3
$[ZnL'Cl_2]$ (**3**)	0.2(3)	0.871(9), 0.870(9)	–	2.590(2)	–
$[ZnL'Br_2]$ (**4**)	26.7(3)	0.873(9), 0.879(9)	–	2.839(2)	–
$Ph_2P(O)C(Ph)NH$-*pbt* [1]	15.4	0.875(13)	1.96(3)	2.685(4)	140(3)
$Ph_2P(O)C(2\text{-furanyl})NH$-*pbt* [1]	15.3	0.872(13)	1.94(2)	2.708(4)	146(4)
$Ph_2P(O)C(4\text{-pyridyl})NH$-*pbt* [1]	14.0	0.879(14)	1.93(5)	2.680(9)	142(7)
Ph_2PNH-*pbt* [2]	13.8	0.850(13)	2.009(15)	2.7167(16)	140.2(15)
$PhP(NH\text{-}pbt)_2$ [2]	3.4	0.871(9)	1.950(13)	2.6944(17)	142.6(16)
	4.1	0.871(9)	2.025(13)	2.7513(17)	140.1(16)
$\{PhP(NH\text{-}pbt)\}_2N$-*pbt* [2]	1.3	0.873(9)	1.941(15)	2.669(2)	139.9(18)
	1.2	0.875(9)	1.956(15)	2.694(2)	141.2(18)
NH_2-*pbt*·0.5DMF [3]	4.2	0.88	2.09	2.751(7)	131.1
	1.6	0.88	2.03	2.679(11)	129.5
NMeH-*pbt* [4]	4.4	0.86	2.03	2.715(2)	135.8
	4.2	0.86	2.04	2.712(2)	134.6

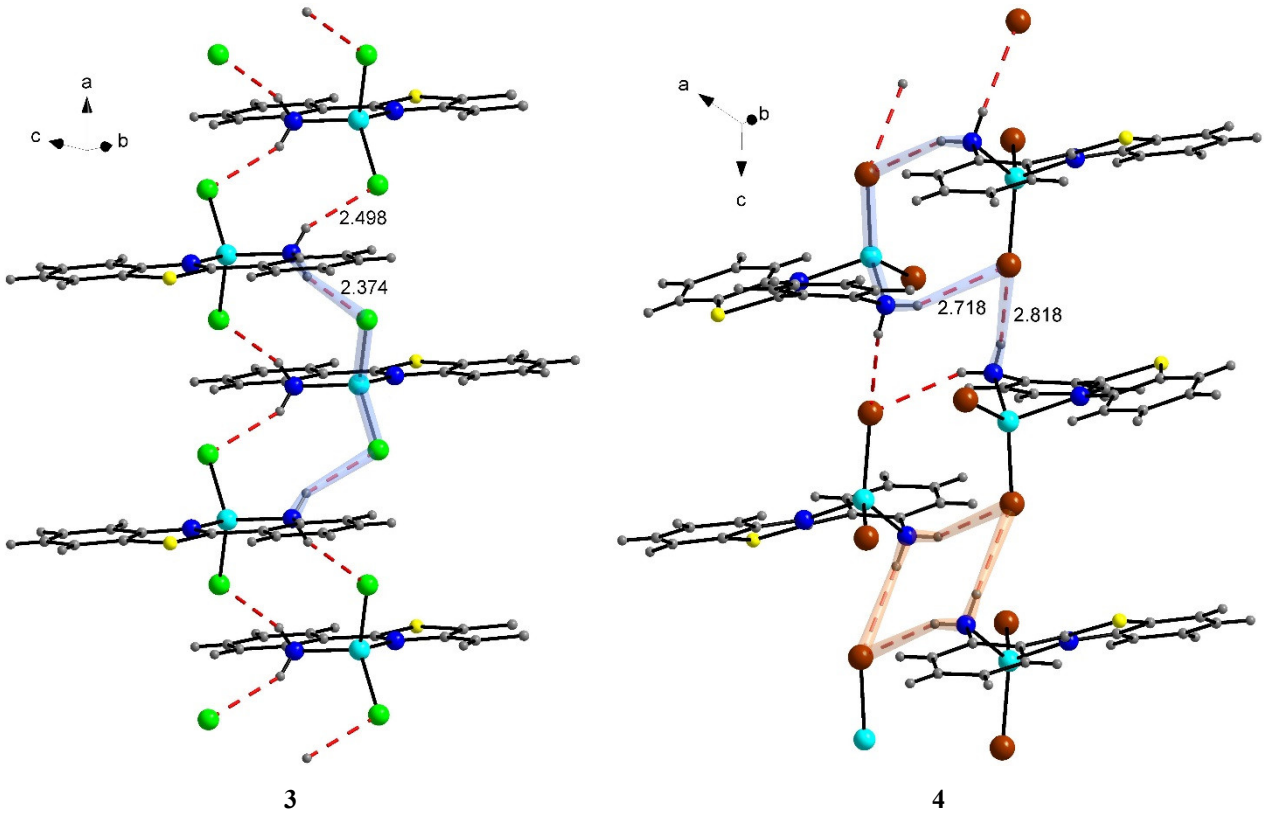

Figure S5. Hydrogen bond network in $[ZnL'Cl_2]$ (**3**) and $[ZnL'Br_2]$ (**4**). Hydrogen bonds are shown as red dashed lines, and H···Hal distances are specified. Chain- and ring-like graph sets of the hydrogen bonds are marked blue and orange, respectively.

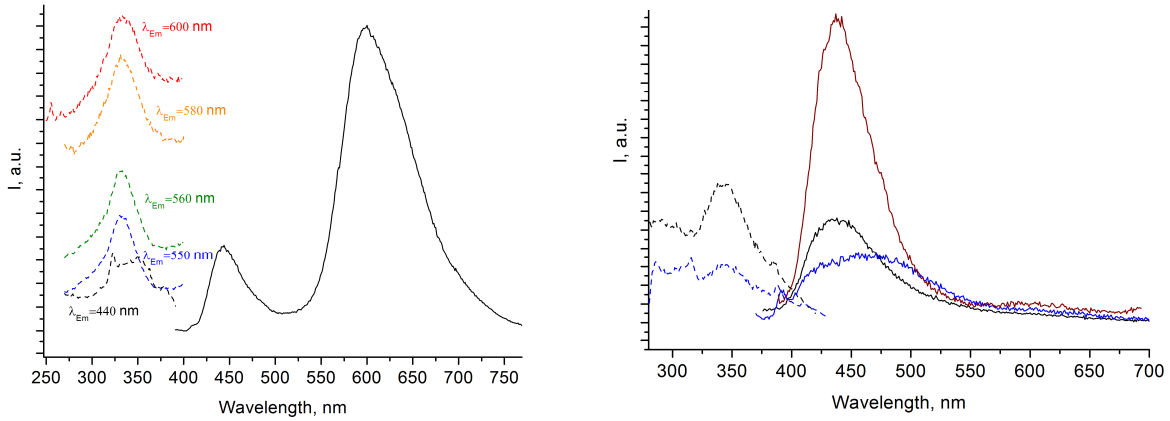

(a) (b)

Figure S6. (**a**) Excitation spectra at different emission wavelengths (dashed lines), and the emission spectrum of solid [Zn(L)$_2$Br$_2$] (**2**). The spectra of solids PCNH-*pbt* and **1** reveal the same tendencies. (**b**) Excitation (dashed lines) and emission (solid lines) spectra of PCNH-*pbt* in tetrahydrofuran (black lines) and toluene (blue lines) solutions with the concentration of $2 \cdot 10^{-5}$M. The emission spectrum of PCNH-*pbt* in tetrahydrofuran solution with the concentration of 10^{-3}M (brown line).

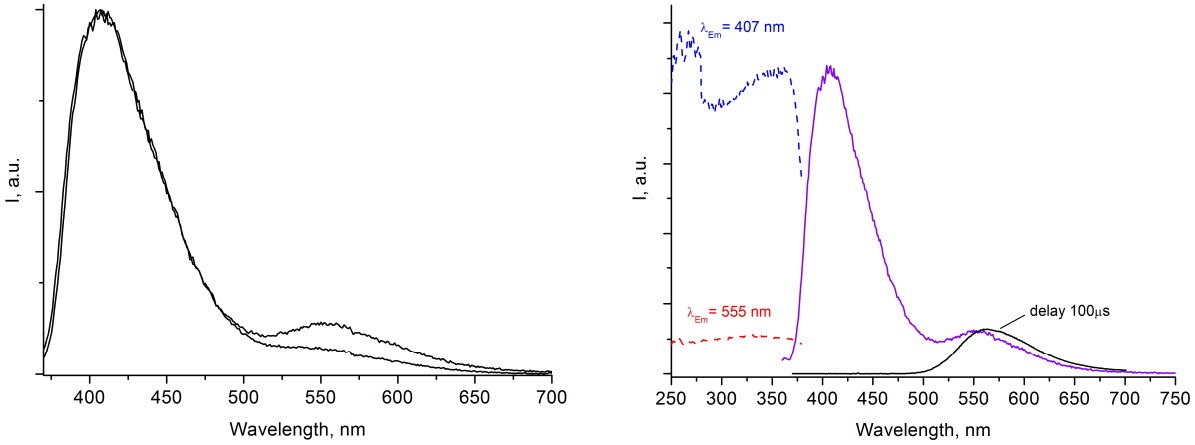

(a) (b)

Figure S7. (**a**) Normalized emission spectra of different solid samples of [ZnL'Br$_2$] (**4**) at excitation wavelength of 350 nm. (**b**) Excitation (blue and red dashed lines) and emission (solid violet and brown lines) spectra, and normalized afterglow emission spectrum after the delay of 100μs (solid black line) of [ZnL'Br$_2$] (**4**). Compound **3** shows similar afterglow.

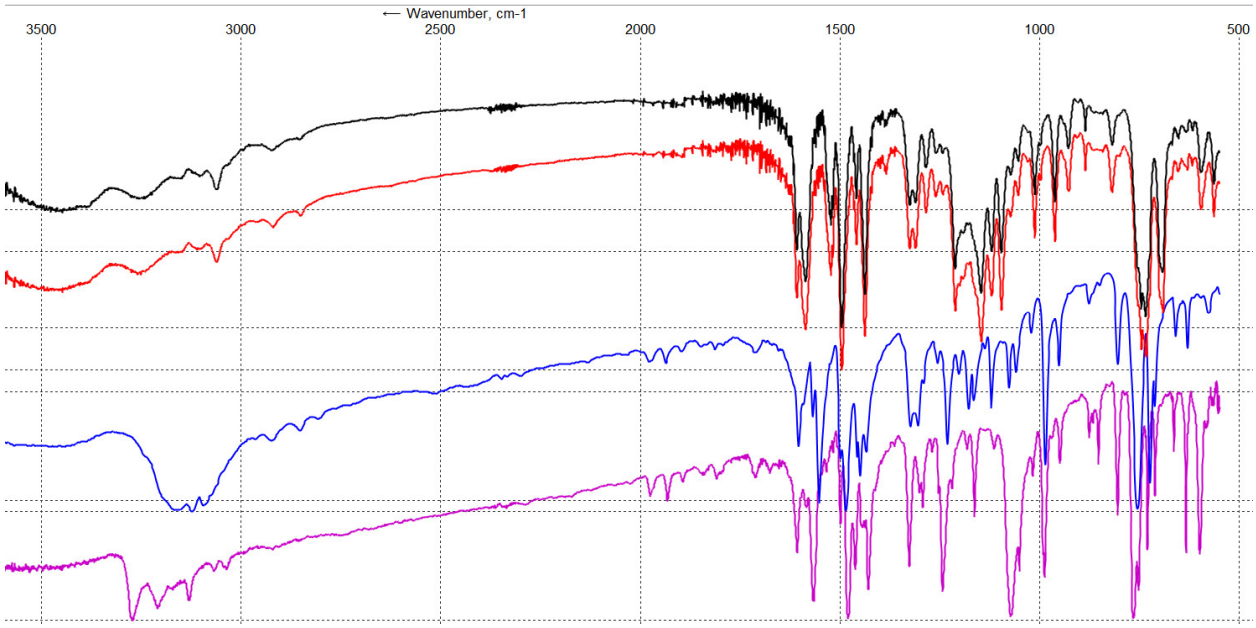

Figure S8. IR spectra of $[Zn(L)_2Cl_2]$ (**1**, black) $[Zn(L)_2Br_2]$ (**2**, red), $[ZnL'Cl_2]$ (**3**, blue) and $[ZnL'Br_2]$ (**4**, magenta).

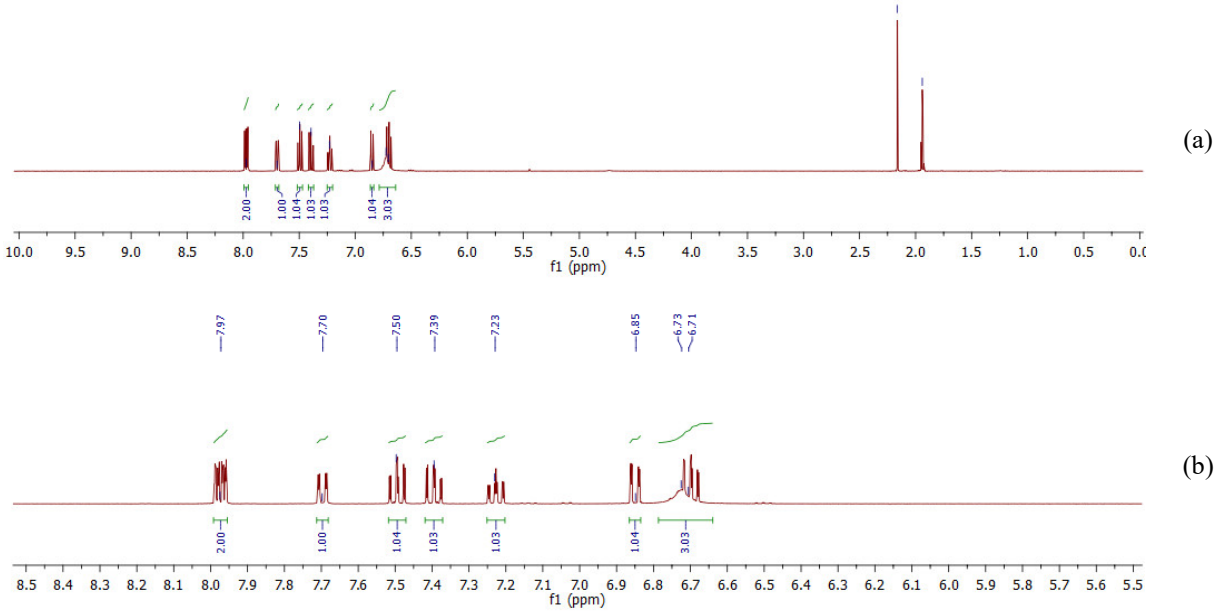

Figure S9. ^{1}H NMR spectrum (400 Mz) of NH_2-*pbt* in CD_3CN (reference peaks at 2.16 and 1.94 ppm) in the range of 0–10 ppm (**a**) and in the range of 5.5–8.5 ppm (**b**).

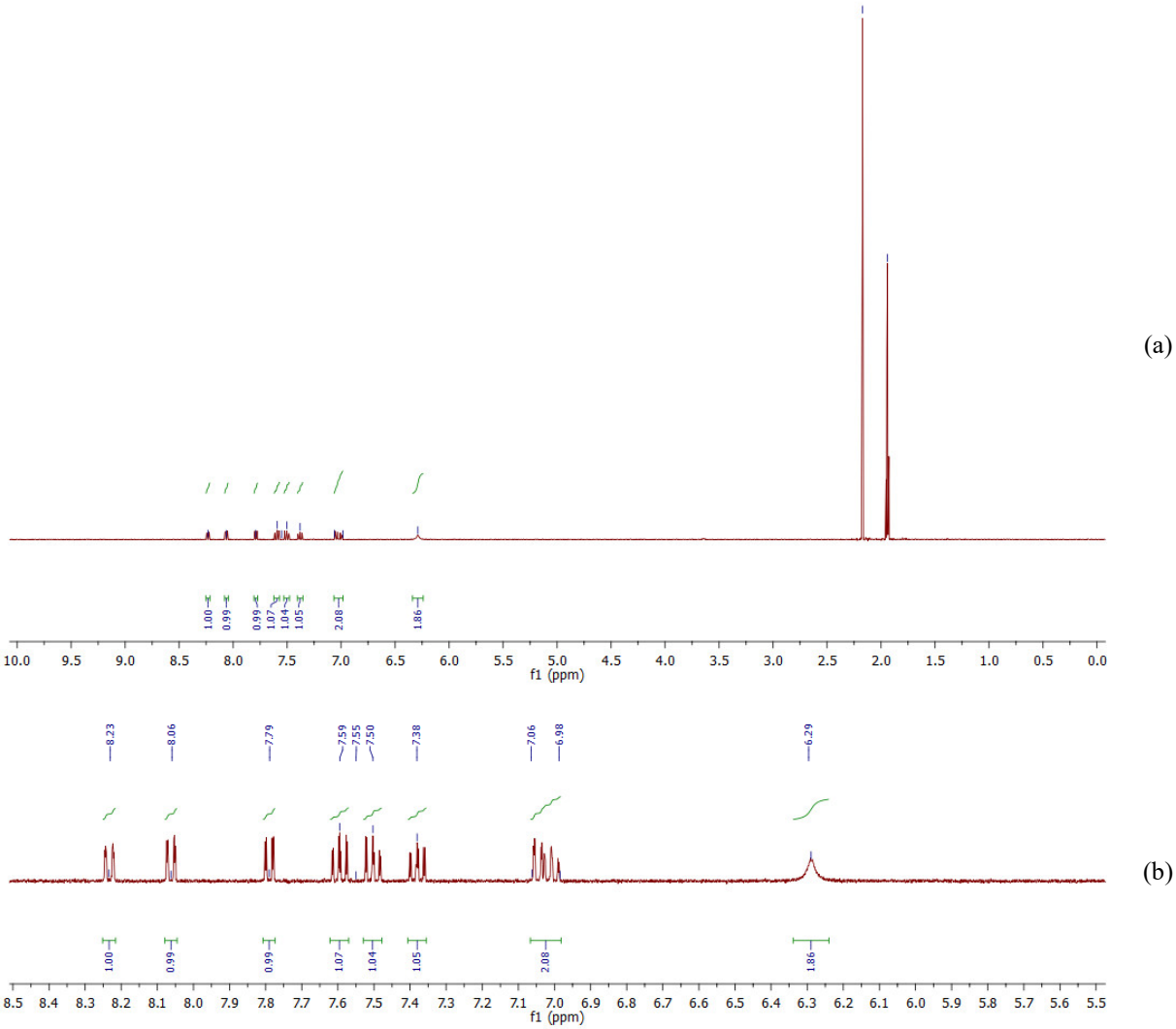

Figure S10. ^{1}H NMR spectrum (400 Mz) of [ZnL′Cl$_2$] (**3**) in CD$_3$CN (reference peaks at 2.16 and 1.94 ppm) in the range of 0–10 ppm (**a**) and in the range of 5.5–8.5 ppm (**b**).

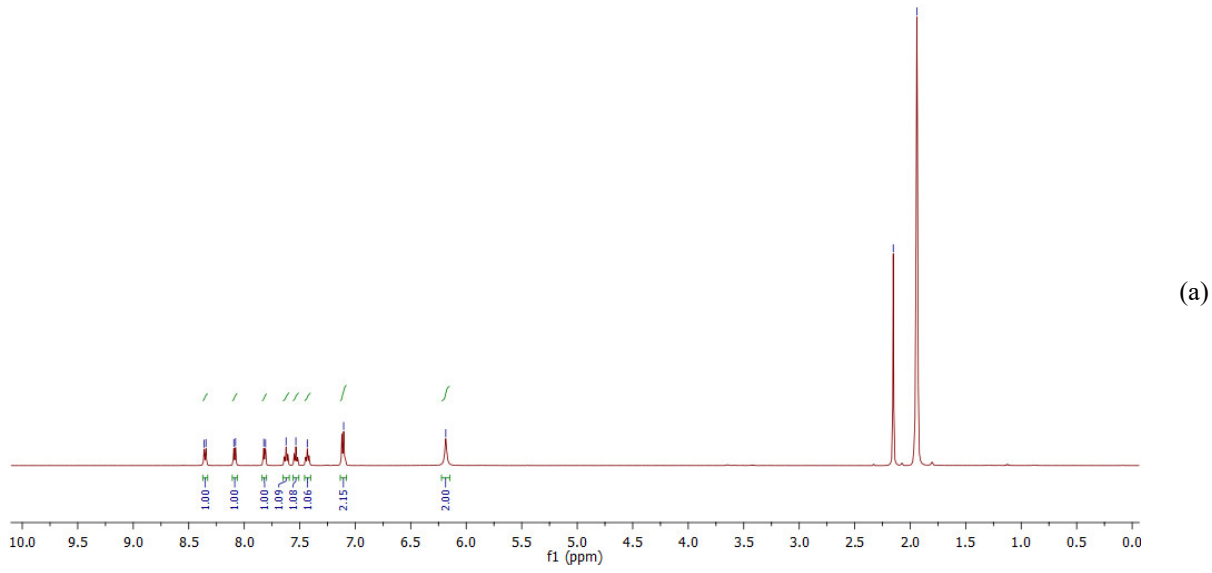

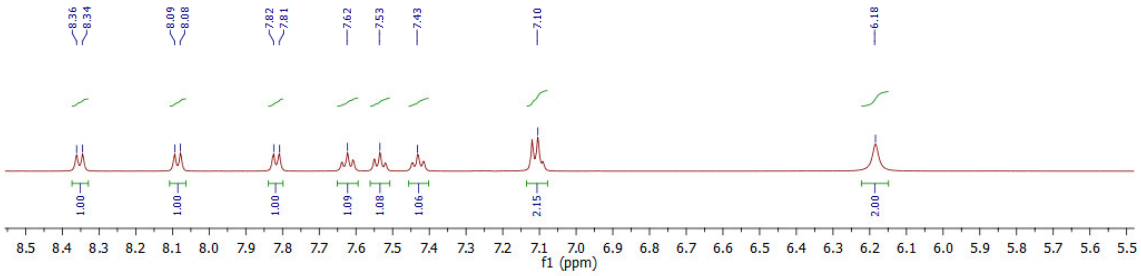

(b)

Figure S11. ^{1}H NMR spectrum (400 Mz) of [ZnL′Br$_2$] (**4**) in CD$_3$CN (reference peaks at 2.16 and 1.94 ppm) in the range of 0–10 ppm (**a**) and in the range of 5.5–8.5 ppm (**b**).

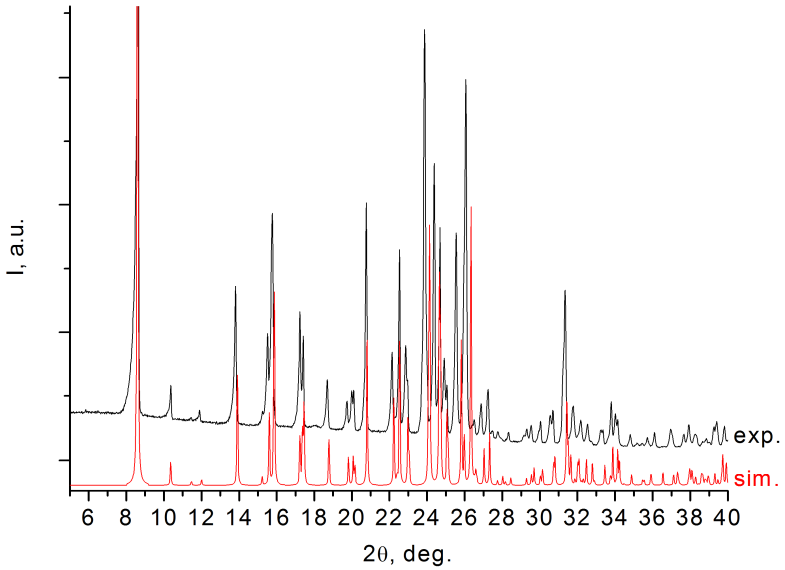

Figure S12. Simulated (red) and experimental (black) powder XRD patterns for the compound [ZnL′Cl$_2$] (**3**; CuKα1 radiation).

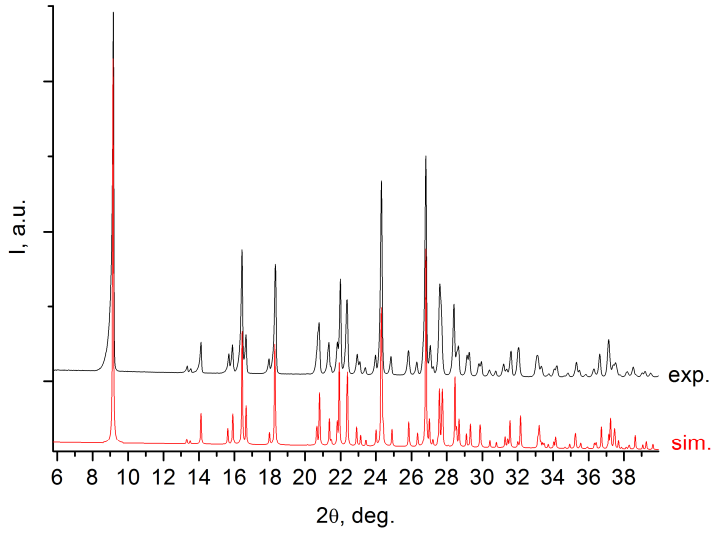

Figure S13. Simulated (red) and experimental (black) powder XRD patterns for the compound [ZnL′Br$_2$] (**4**; CuKα1 radiation).

[1] CCDC numbers 2166671-2166673. T. S. Sukhikh, D. S. Kolybalov, R. M. Khisamov, S. N. Konchenko, Journal of Structural Chemistry, 2022. In press. https://doi.org/10.26902/JSC_id97834

[2] R. M. Khisamov, A. A. Ryadun, T. S. Sukhikh, S. N. Konchenko, Molecular Systems Design & Engineering, 2021, 6, 1056. https://doi.org/10.1039/D1ME00117E

[3] CSD Communication, 2017, Refcode BEFJEE. https://doi.org/10.5517/ccdc.csd.cc1lsw19

[4] T. K. Venkatachalam, G. K. Pierens, P. V. Bernhardt, D. C. Reutens, Magnetic Resonance in Chemistry, 2015, 53, 448. https://doi.org/10.1002/mrc.4228